

A moving target: trade-offs between maximizing carbon and minimizing hydraulic stress for plants in a changing climate

Gregory R. Quetin¹ , Leander D. L. Anderegg² , Indra Boving²  and Anna T. Trugman¹ 

¹Department of Geography, University of California, Santa Barbara, CA 93016, USA; ²Department of Ecology, Evolution, and Marine Biology, University of California, Santa Barbara, CA 93016, USA

Summary

Author for correspondence:
Gregory R. Quetin
Email: gquentin@ucsb.edu

Received: 29 January 2024
Accepted: 27 August 2024

New Phytologist (2024)
doi: [10.1111/nph.20127](https://doi.org/10.1111/nph.20127)

Key words: acclimation, climate change, CO₂ fertilization, leaf area, net carbon gain, plant water stress, tree canopy.

- Observational evidence indicates that tree leaf area may acclimate in response to changes in water availability to alleviate hydraulic stress. However, the underlying mechanisms driving leaf area changes and consequences of different leaf area allocation strategies remain unknown.
- Here, we use a trait-based hydraulically enabled tree model with two endmember leaf area allocation strategies, aimed at either maximizing carbon gain or moderating hydraulic stress. We examined the impacts of these strategies on future plant stress and productivity.
- Allocating leaf area to maximize carbon gain increased productivity with high CO₂, but systematically increased hydraulic stress. Following an allocation strategy to avoid increased future hydraulic stress missed out on 26% of the potential future net primary productivity in some geographies. Both endmember leaf area allocation strategies resulted in leaf area decreases under future climate scenarios, contrary to Earth system model (ESM) predictions.
- Leaf area acclimation to avoid increased hydraulic stress (and potentially the risk of accelerated mortality) was possible, but led to reduced carbon gain. Accounting for plant hydraulic effects on canopy acclimation in ESMs could limit or reverse current projections of future increases in leaf area, with consequences for the carbon and water cycles, and surface energy budgets.

Introduction

Forests cover 31% of the Earth, dominate both the terrestrial carbon sink and aboveground carbon storage, and play a major role in the hydrological cycle through transpiring c. 40% of land rainfall back to the atmosphere (Schlesinger & Jasechko, 2014; Yang *et al.*, 2023). However, increasingly arid conditions driven by climate change have increased forest stress and already manifested in elevated mortality rates world-wide (Allen *et al.*, 2015). Understanding how forests acclimate to (or die from) changing climate conditions is critical for both basic understanding of physiological and ecological function and for conservation and management practices as humans pursue climate change adaptation.

Trees can modulate function in response to changing environmental conditions through a number of mechanisms. Stomata are rapid responders, on the order of seconds to minutes, that open and close to both regulate CO₂ diffusion into the leaf and water loss out of the leaf in response to changing environmental conditions throughout a day and over the course of a growing season. On climate change-relevant scales – longer than a growing season but shorter than the lifetime of a tree – carbon allocational changes have the potential to alleviate stress and allow for acclimation to novel environmental conditions (Hartmann *et al.*, 2020). Carbon allocation to tree crowns (i.e. leaf area) is

one important lever in the context of increasing aridity and concomitant increases in tree hydraulic stress. Total tree leaf area affects both plant carbon assimilation and hydraulic stress by regulating photosynthetic leaf area, leaf respiration costs, and the amount of water that flows through the tree and that is lost to the atmosphere through leaves. Analyses over the last several decades suggest that increasing the amount of carbon going to leaf area increases gross primary productivity (GPP) (Q. Li *et al.*, 2018; Chen *et al.*, 2019). However, increases in leaf area are not always beneficial. For example, in particularly dry years or in seasonally dry forests, trees shed leaves to avoid high water demand and associated stress (Pivovaroff *et al.*, 2016; Wolfe *et al.*, 2016; Levionnois *et al.*, 2020; Nadal-Sala *et al.*, 2021; Sabot *et al.*, 2022). Additionally, across a climate gradient of aridity, trees in more arid regions have lower total leaf areas (relative to their stem and root tissues) compared with the same species in areas where water is more abundant (Eagleson, 1982; Baldocchi & Xu, 2007; Pivovaroff *et al.*, 2014; Xu *et al.*, 2016).

First principles (Franklin *et al.*, 2012; Quetin *et al.*, 2023) and observations (Wolfe *et al.*, 2016; Levionnois *et al.*, 2020) both indicate that allocation is critical in shaping plant responses to climate. However, exactly how plants adjust allocation to the environment is still a major unknown (Hartmann *et al.*, 2018). This uncertainty is reflected in the diversity of approaches used to

represent carbon allocation in terrestrial ecosystem models, where approaches range from a prescribed allocation of carbon to the leaves, stems, roots, and nonstructural carbohydrate reserves of the plant based on fixed coefficients, to more complex theory that balances the benefits from investing carbon in different plant organs based on fitness (Arora & Boer, 2005; De Kauwe *et al.*, 2014).

One path forward in understanding tree carbon partitioning is through a lens of optimality. We expect that trees evolve to allocate carbon optimally to maximize fitness (Hölttä *et al.*, 2011; Franklin *et al.*, 2012, 2020; Wolf *et al.*, 2016; Deans *et al.*, 2020; H. Wang *et al.*, 2020; Harrison *et al.*, 2021; Joshi *et al.*, 2022). This optimality involves both genetically determined differences in allocation (e.g. macroevolutionary differences among related species that inhabit different environments (Sanchez-Martinez *et al.*, 2020)), and plastic changes that allow an individual to tailor its allocation to its growth environment (Rowland *et al.*, 2023). While optimization of the leaf area to stem area of a tree has been suggested as a potential improvement in modeling carbon allocation (Trugman *et al.*, 2019), it is a major unknown exactly what optimality criterion is the best proxy for the maximization of fitness, particularly whether increased fitness is linked to increased carbon gain, hydraulic stress mediation, or some combination of the two. For long-lived trees, plastic optimization or acclimation over the course of years is particularly relevant for understanding responses to climate change, but particularly difficult to disentangle observationally thanks to the difficulty of measuring fitness in trees.

Here, we hypothesize two potential endmember allocation strategies for climate change acclimation based on principles of optimality. In one strategy, trees allocate carbon to leaf area to maximize net primary productivity (NPP) ('max carbon gain'). In the other strategy, trees allocate carbon to leaf area to avoid increases in stress beyond historical levels ('stress avoidance') (Fig. 1). Maximizing carbon gain, a common proxy for overall plant fitness (Mooney & Gulmon, 1979), may be the riskier approach to allocation as it does not explicitly account for the possible increase in hydraulic damage that can reduce a tree's function, decrease carbon assimilation, and eventually result in mortality (Anderegg *et al.*, 2015). 'Stress avoidance' is the less risky approach and provides acclimation that explicitly avoids increased hydraulic stress, but may lead to missing out on NPP of the 'max carbon gain' strategy.

To test the impact of these two hypotheses and investigate the trade-offs between the 'max carbon gain' and 'stress avoidance' strategies, we use a trait-based model of tree gas exchange that simulates an individual tree, with hydraulic transport and the leaf carbon allocation determined by these two optimization strategies (Trugman *et al.*, 2019; Quetin *et al.*, 2023). We ask (1) How much carbon do trees miss out on when they optimize for stress avoidance relative to carbon maximization, considering elevated aridity and CO₂ with future climate change? (2) How do projections of tree leaf area change under our endmember allocation strategies compare to leaf area change in process-based Earth system models (ESMs)? (3) Can observed physiological diagnostics such as measured CO₂ fertilization be used to distinguish

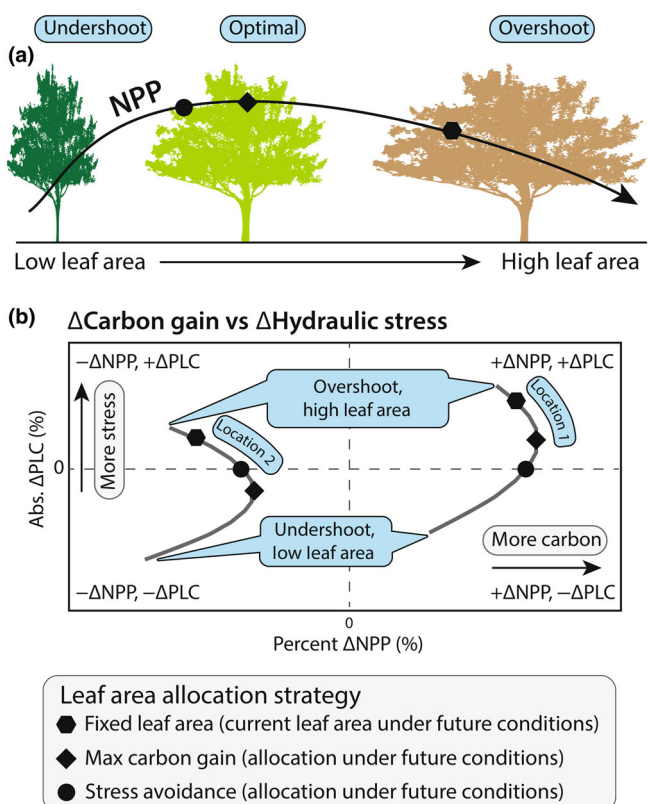


Fig. 1 Carbon assimilation and hydraulic stress are shaped by climate and linked through canopy demand for water to be supplied from the soil through shoots and roots. (a) Increasing leaf area (with a fixed tree stem) can potentially increase net primary productivity (NPP) but also increase water loss and water potential. (b) Altering the carbon allocation to leaf area results in a curvilinear change in percent loss of hydraulic conductivity (PLC, a measure of hydraulic damage) and NPP. Gray lines represent the sweep of Δ PLC and Δ NPP relative to current conditions that result from varying leaf area. The two different lines illustrate different locations with different underlying tree communities, different climates, and experiencing different climate change. Present-day allocation almost always results in nonmaximum NPP and increased PLC in the future (fixed leaf area), but different endmember allometric strategies that maximize carbon ('max carbon gain') and avoid increased stress ('stress avoidance') land on different portions of this line (see key).

between allocation strategies and improve our understanding of plant function?

Materials and Methods

Hydraulic Optimization Theory for Tree and Ecosystem Resilience model

The Hydraulic Optimization Theory for Tree and Ecosystem Resilience (HOTTER) model is a trait-based physiological tree model that represents individual trees with an explicit representation of plant hydraulics. The model consists of tree leaf area, stem, and roots that span the soil-atmosphere continuum to conduct water from the soil to the canopy (Supporting Information Fig. S1). Respiration rates are organ specific to leaves, xylem,

phloem, and roots based on observed rates and temperature sensitivities (Trugman *et al.*, 2019; Quetin *et al.*, 2023) (Eqns S21–S28). The leaf-level stomatal behavior employs a cost-gain model that optimizes the ‘cost’ of percent loss of conductivity (hydraulic damage, set by the plant’s hydraulic vulnerability curve) with the ‘benefit’ of carbon assimilation as per the Stomatal Optimization Based on Xylem Hydraulics model (Eller *et al.*, 2018) (Eqns S8–S20). Transpiration is calculated as diffusion from the interior of the leaf, based on the stomatal conductance and atmospheric vapor pressure deficit (VPD) (Eqns S13, S29). Leaf-level carbon assimilation and transpiration are scaled to the canopy with a linear relationship with tree leaf area (Eqns S1–S7, S30, S31; Methods S1; Notes S1). The HOTTER model responds to daily atmospheric CO₂ concentrations (CO₂, ppm), temperature (T , °C), VPD (Pa), and soil water potential (Ψ_{soil} , MPa). Carbon gain and hydraulic stress are prognostic based on model equations, traits, and variations in environmental factors.

The model is based on established theory and has been validated against, among others, the spatial variation of plant structures that govern water demand and supply (i.e. leaf area: sapwood area) (Trugman *et al.*, 2019), carbon use efficiency (Mathias & Trugman, 2022), and mortality patterns across the continental United States (Quetin *et al.*, 2023). An expanded list of model parameters can be found in the Supporting Information along with a full model description (Methods S1, S2; Table S1).

HOTTER plant hydraulic theory and leaf allocation

The impact of tree leaf area in our model is determined by the local environment and the balance of GPP, respiration, and hydraulic stress. Increasing tree leaf area (i.e. the ratio of leaf area to sapwood area, with sapwood area fixed) increases total carbon gain but also increases whole-plant hydraulic stress (diagnosed as percent loss of hydraulic conductivity, PLC) (Fig. S1). As hydraulic stress increases, stomata close, limiting leaf-level productivity and eventually leading to the increased leaf and root respiration surpassing productivity gains (i.e. decreased NPP). The ‘max carbon gain’ leaf area results from the allocation strategy that maximizes the balance between whole-plant productivity and respiration (Fig. S1).

Under future conditions, the resulting leaf area from an allocation strategy may change (Fig. S1b), and we can define mathematically endmember allocation strategies that either maximize tree-level net carbon gain (i.e. NPP) in the new environment or avoid increases in hydraulic stress (i.e. PLC) compared with the historical simulation (noted symbols in Figs 1, S1). Through evolution and acclimation, it is theorized that plants approach a function that maximizes their fitness (Franklin *et al.*, 2020). However, without knowing the exact function that relates physiological performance to maximum fitness we explored two endmember allocation strategies, and a no allocation change ‘control’ strategy, with a focus on the trade-off between carbon gain and hydraulic stress.

The leaf area changes with each strategy are governed by changes in model forcings of atmospheric CO₂ concentrations, VPD, and temperature (T) (for this experiment soil moisture is

held constant). The expected future increase in atmospheric CO₂ concentrations could lead to increased GPP and water use efficiency (productivity per water demand) – creating the potential for increased NPP and reduced hydraulic stress (Ainsworth & Long, 2005; Battipaglia *et al.*, 2013; Franks *et al.*, 2013; Domec *et al.*, 2017; Walker *et al.*, 2021). However, increases in VPD tend to increase water loss from plants and act against CO₂ fertilization by driving stomatal closure to avoid increased stress (Grossiord *et al.*, 2020). Finally, increases in temperature increase the respiration cost of the tree in our model, which favors smaller canopies due to high leaf respiration rates compared with productivity (Fig. S1). These varying trade-offs have the potential to alter the tree leaf area for a given tree, under different environmental conditions (Fig. 1b). Depending on the particular ‘end-member’ allocation strategy and the changing climate, there is the potential for both increases and decreases in leaf area, with subsequent impacts of carbon assimilation and stress (Fig. 1b).

Data sources

The HOTTER model was run for forested regions at 0.25° resolution covering most regions of the contiguous United States, using the environmental data and community/stand attributes of the US Forest Service Forest Inventory & Analysis plots (Gillespie, 1999; Trugman *et al.*, 2020).

Meteorology and atmospheric CO₂ concentrations The meteorological daily input for the HOTTER tree model was a present-day set of data covering a 20-yr time period from 1995 to 2014, and a future scenario covering a 20-yr time period from 2081 to 2100. The meteorology consisted of Ψ_{soil} , T , and VPD for the growing season (Table 1). The Ψ_{soil} was left fixed at present values, given the uncertainty across models in directional changes in soil moisture compared with that of atmospheric CO₂ concentrations, VPD, or T (Yuan *et al.*, 2021) and the indirect effect of soil moisture on vegetation function through the regulation of VPD (Humphrey *et al.*, 2021).

Ecological data The HOTTER model was parameterized with tree height derived from maps of canopy height measured by satellite and a range of P50 values for each model grid cell based on maps of community-weighted mean and the regional minimum and maximum values based US Forest Inventory data (Trugman *et al.*, 2020; Table 2).

Change in leaf area index and GPP from CMIP6 Separate from the downscaled meteorology from CMIP6 (Table 1), the leaf area index (LAI) from 20 models and GPP projections from 17 models (Table S2) included in CMIP6 suite of models for the ‘medium’ SSP3-7.0 scenario were used for comparison with the HOTTER endmember allocation strategy estimates (Eyring *et al.*, 2016). The LAI and GPP for CMIP6 model data were downloaded using from Google public storage – <https://storage.googleapis.com/cmip6/pangeo-cmip6.json> – using Pangeo in Python as documented online as the Google Cloud CMIP6 Public Data: Basic Python Example (<https://gallery.pangeo.io/repos/>

Table 1 Meteorology for the present and future runs.

Name	Time	Lat/Lon res	Time res	Variables	CO ₂ (ppm) ¹	Source
Present	1995–2014	0.25°	Daily	Ψ _{soil} , T, VPD	370	GLDAS Catchment Land Surface Model L4 daily 0.25 × 0.25-degree GRACE-DA1 V2.2 (GLDAS_CLSM025_DA1_D_2.2) (Li <i>et al.</i> , 2019, 2020)
Future	2081–2100	Various, regrid to 0.25°	Daily	T, VPD	753	Future daily values are modeled as present-daily values plus the average monthly change in climate for SSP3-7.0 from a selection of Coupled Model Intercomparison Project Phase 6 (CMIP6) ²

¹CO₂ was held constant during each experimental time periods as averages taken from observations at Mauna Loa (370 ppm) (Keeling *et al.*, 2009, 2017) for the present day and taken from the CMIP6 SSP 3–7.0 emissions scenario for the future (753 ppm) (O’Neill *et al.*, 2016).

²Models used in creating the average meteorological change were: ACCESS-CM2, ACCESS-ESM1-5, CanESM5-CanOE, MIROC-ES2L, MPI-ESM1-2-LR, and MRI-ESM2-0THE. Downscaled model products publicly available from (Anderegg *et al.*, 2022).

Table 2 Height and P50 values processed as detailed in (Quentin *et al.*, 2023).

Name	Observation timeframe	Lat/Lon res	Source
Height	2019	0.00025°, regrid to 0.25°	Global Ecosystem Dynamics Investigation (GEDI) instrument and processed by the Global Land Analysis and Discover team at the University of Maryland (Potapov <i>et al.</i> , 2021)
P50	2008–2018	Individual plots gridded to 0.25°	The maps derived from (Trugman <i>et al.</i> , 2020)

pangeo-gallery/cmip6/basic_search_and_load.html). The growing season (June, July, and August) mean was selected for all models, and each was regridded to 0.25°.

Experimental setup

We ran five sets of experiments to understand the impacts of different allocation strategies on plant function. The first run used 20 yr of present-day climate conditions and retrieved a single leaf area for each location – including location-specific traits – that maximized mean NPP for the full run (‘present-day run’). While real-world leaf area varies on an interannual basis in response to climate variation and legacy effects, a single leaf area for the 20-yr span captures the long-term changes due to climate change, the aim of this study. The second run used 20 yr of future climate conditions and the leaf area from the ‘present-day run’ (‘fixed leaf area’). The third run used 20 yr of future climate conditions and retrieved a leaf area for each location that maximized NPP as in the ‘present-day run’ but with future climate (‘max carbon gain’). The fourth run used 20 yr of future climate and retrieved the leaf area such that $PLC_{\text{present}}^{90\text{th}} - PLC_{\text{future}}^{90\text{th}} = 0$, where $PLC^{90\text{th}}$ is the 90th percentile of the daily PLC values that represent relatively stressed conditions (‘stress avoidance’) (90th percentile refers to the distribution of daily PLC rather than the PLC units of percent) (Table 3). Notably, the ‘stress avoidance’ leaf area allocation strategy is partially dependent on the max carbon gain hypothesis as it is defined as holding $PLC_{\text{future}}^{90\text{th}}$ constant relative to the ‘present-day run’ where leaf area was chosen to maximize mean NPP for the present day. Finally, we tested the effect of the observed acclimation of canopy efficiency or $V_{c,\text{max}25}$ (see Eqns S42–S44) to increased atmospheric concentrations of CO₂ by applying a 20% reduction in $V_{c,\text{max}25}$ following a ‘max carbon

Table 3 Endmember allocation strategies investigated.

Name	Description
Fixed leaf area	Allocation strategy to maximize NPP under present-day conditions
Max carbon gain	Allocation strategy to maximize NPP under future conditions
Stress avoidance	Allocation strategy to avoid change in the 90 th percentile PLC between future and present conditions with an allocation strategy of maximizing NPP

gain’ allocation strategy (‘ $V_{c,\text{max}25}$ CO₂ acclimation’). In practice, the maximum NPP for ‘present-day run’ and ‘max carbon gain’ was found using `scipy.optimize` while the ‘stress avoidance’ endmember allocation strategy was calculated by incrementing the tree leaf area around the future ‘max carbon gain’ optimum to match the no PLC change condition. For a few points, the resolution of the increment used in ‘stress avoidance’ resulted in a small remainder of negative change in PLC in conditions where ‘max carbon gain’ already resulted in reduced hydraulic stress in the future (Fig. 2c).

For computational efficiency, 1500 grid points (i.e. locations) were randomly chosen from the 9000 grid points in the full map to test the endmember allocation strategy. The number of points were chosen to represent a statistically indistinguishable – per the Mann–Whitney test – distribution of NPP from the full 9000 grid points run for present-day conditions.

We performed an additional run forcing HOTTER with an ESM-predicted leaf area change under future conditions, which allowed for a complimentary investigation of the potential hydraulic stress impacts that could be realized with ESM-predicted LAI change (as hydraulics are not present in the

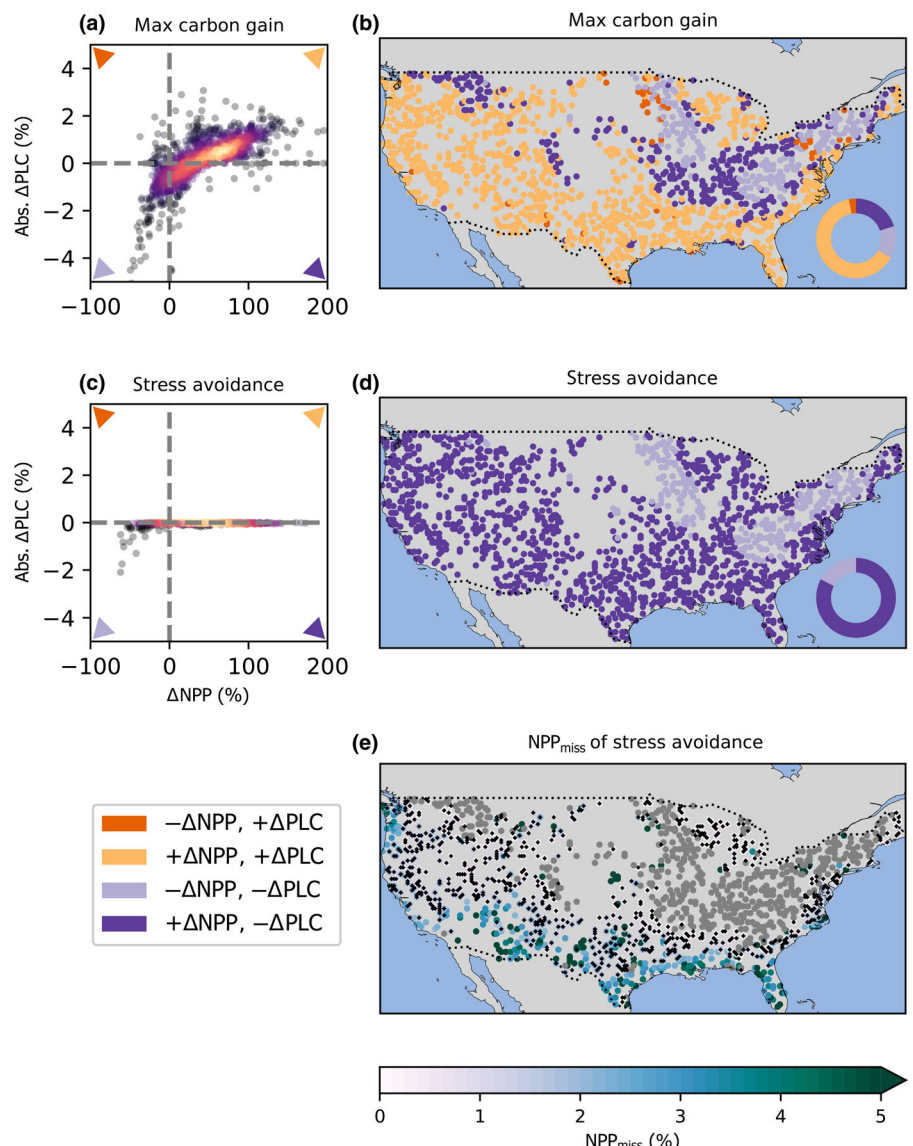


Fig. 2 Maximizing carbon gain under future climate change increases water stress in many regions. Change in water stress (percent loss of conductance, PLC) and percent change in carbon gain (net primary productivity, NPP) with an allometric strategy that (a) maximizes NPP or (c) avoids change in water stress, (b, d) map and pie chart of which quadrant each grid point falls in for (b) 'max carbon gain' strategy and (d) 'stress avoidance' strategy, and (e) a map of the percent carbon missed out on by avoiding increased water stress rather than maximizing carbon gain (NPP_{miss}). Gray points in (e) are the points where water stress decreased following a 'max carbon gain' strategy (495 of 1500 points). Black diamonds in (e) are stippling that denotes points where the NPP_{miss} is statistically uncertain (NPP_{miss} less than the SE of the daily variation) (693 of 1500 points).

vast majority of ESMs). For this experiment run, we used the fractional change in LAI from the mean of the CMIP6 models as a boundary condition.

For each leaf area allocation strategy, we ran a 'total' run where both future climate and future atmospheric concentrations of CO₂ was applied and a 'CO₂ only' run where climate is held at present-day conditions but atmospheric concentrations of CO₂ are increased. These CO₂ only runs were specifically for analysis of the CO₂ fertilization effect without climate change but with the effect of allocation strategies (allocation strategies respond to both future climate and atmospheric CO₂ concentrations), 'fixed leaf area', and ESM-predicted leaf area. Previous work with full factorial runs with 'fixed leaf area' – including separate runs for VPD, temperature, and atmospheric concentrations of CO₂ – found the CO₂ and VPD to be primary drivers of change across diverse regions (Quentin *et al.*, 2023).

Carbon missed through stress avoidance and uncertainty The carbon missed out on due to the 'stress avoidance' strategy was calculated as the difference between the 'stress avoidance' strategy's mean daily NPP and the 'max carbon gain' strategy's mean daily NPP, Eqn 1:

$$\text{NPP}_{\text{miss}} = \left(\frac{\text{NPP}_{\text{max carbon gain}} - \text{NPP}_{\text{stress avoidance}}}{\text{NPP}_{\text{max carbon gain}}} \right) \times 100 \quad \text{Eqn 1}$$

The uncertainty of the carbon missed was calculated based on the SE from the SD of the daily variance across the 1840 d of each model run (Eqn 2). This uncertainty represents the statistical strength of the difference between NPP due to allocation strategies (i.e. NPP_{miss}) given the simulated daily variance of NPP, Eqn 2:

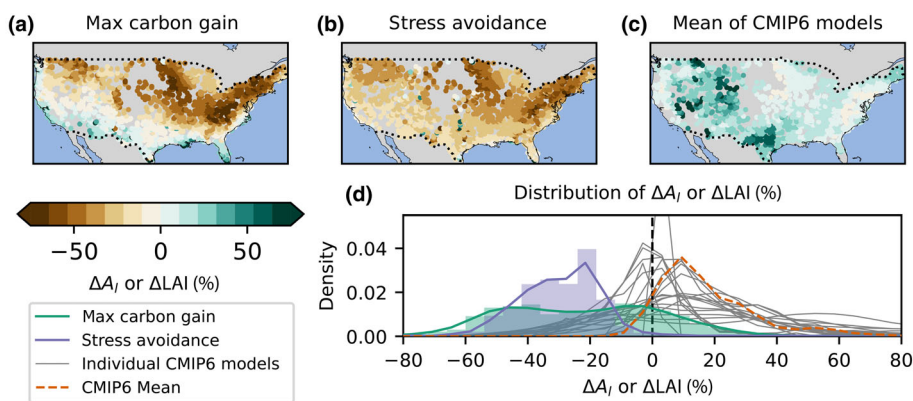


Fig. 3 Percent change in future leaf area varies across endmember allocation strategies and largely diverges from CMIP6. The percent change in future leaf area for (a) 'max carbon gain' endmember allocation strategy, (b) 'stress avoidance' endmember allocation strategy, and (c) the mean of CMIP6 models. (d) Histogram of the leaf area change for endmember allocation strategies, and leaf area index change for the CMIP6 model mean, and individual CMIP6 models.

$$S.E. = \left(\frac{\sigma_{npp, \text{max carbon gain}} + \sigma_{npp, \text{stress avoidance}}}{|NPP_{\text{max carbon gain}} - NPP_{\text{stress avoidance}}|} \right) \times \frac{1}{1840} \quad \text{Eqn 2}$$

where $\sigma_{npp,x}$ is the SD of the daily variance for each endmember allocation strategy. All points in Fig. 2d are stippled in black where $S.E. > NPP_{\text{miss}}$.

Calculating CO₂ fertilization The CO₂ fertilization effect was calculated as the ratio of the log of the change in GPP and atmospheric CO₂ concentrations (Walker *et al.*, 2021), Eqn 3:

$$\beta = \log\left(\frac{GPP_{\text{future}}}{GPP_{\text{present}}}\right) / \log\left(\frac{C_{\text{a,future}}}{C_{\text{a,present}}}\right) \quad \text{Eqn 3}$$

where β is the CO₂ fertilization effect and C_{a} is the atmospheric concentration of CO₂.

Results

The effect of avoiding future stress on net primary productivity

Across the majority of the continental United States, HOTTER projected increased NPP with climate change for both endmember allocation strategies. Specifically, NPP for the 'max carbon gain' strategy increased over 84% of forested areas and for the 'stress avoidance' strategy over 83% of forested areas (Fig. 2). However, while 'stress avoidance' maintained increased future NPP (i.e. positive change in NPP in both 'max carbon gain' and 'stress avoidance' strategies) in 95% of locations compared with 'present-day', it did result in reduced NPP compared with the 'max carbon gain' strategy in many places. Using HOTTER we quantified the NPP missed out on (NPP_{miss}) from following an allocation strategy of 'stress avoidance' compared with 'max carbon gain'. We found that there was an NPP_{miss} of up to 26% (first percentile of points) of future NPP at some locations (Fig. 2c), but that the integrated NPP_{miss} across the entire United

States for 'stress avoidance' only reduces the continental scale NPP by 1% because there was a majority of locations where the difference was minimal (Fig. 2d). In contrast to both endmember allocation strategies, no acclimation in leaf area under future conditions (i.e. 'fixed leaf area') leads to broad areas of NPP_{miss} above 40% that are also well above the carbon missed of 'stress avoidance' and include areas of negative absolute NPP (Figs S2, S3).

The 'max carbon gain' strategy increased NPP along with increased hydraulic stress in 64% of the locations analyzed (i.e. top right quadrant in Fig. 2a). Only 20% of locations resulted in increased NPP and decreased stress with projected climate change (e.g. bottom right quadrant in Fig. 2a).

The effect of climate change on plant carbon assimilation and stress is also dependent on the species and functional diversity of the ecosystem. To compare this 'functional trait' effect with the endmember allocation effect, we calculated the NPP_{miss} of 'stress avoidance' for the region's least drought-vulnerable and most drought-vulnerable species from (Trugman *et al.*, 2020). We found that the difference in NPP_{miss} between functional trait extremes was similar to the magnitude of NPP_{miss} for 'stress avoidance' (using the community-weighted mean P50) across many locations (trait effect of at least 10% of NPP_{miss} for 75% of the points) (Fig. S4).

Leaf area change predicted by endmember hydraulic allocation strategies with comparison to Earth system models

Extensive leaf area decreases are predicted by HOTTER for both 'max carbon gain' and 'stress avoidance' strategies. When trees allocated for 'max carbon gain', leaf area decreased between historical and future climates for all but 21% of the locations (Figs 3a, S5), with positive values concentrated along the West Coast and Southern edge of the United States. In an experiment where $V_{c,\text{max25}}$ was reduced by 20%, representing potential acclimation of $V_{c,\text{max25}}$ to increased atmospheric concentrations of CO₂ (e.g. Ainsworth & Long, 2005; see the Materials and Methods section), the predicted decrease in leaf area following a 'max carbon gain' allocation strategy was reduced. However, the overall trajectory of leaf area decrease reversed in a limited number of geographies (Fig. S6). Following a 'stress avoidance' allocation

strategy resulted in model-projected decreases in leaf area in all but 2% of locations under future conditions (Fig. 3b). The different spatial patterns for the two endmember allocation strategies are primarily explained by present-day VPD and the magnitude of the change in VPD in the future (Notes S2; Figs S7–S9; Tables S3, S4).

In contrast to the widespread leaf area decrease emergent from the endmember allocation strategies in HOTTER, ESMs generally predicted widespread LAI increases in the future. Only five ESMs predicted an LAI decrease in more than half of grid points (Table S2). However, while there was large agreement across ESMs that LAI increases in the future across most of the United States, the variance across models was large (on the order of the mean change) and there was a strong heterogeneity across space and across models in LAI changes (Figs 3, S10, S11). The largest CMIP6 mean model LAI increases ($> +50\%$) were predicted in the Mountain West region and central Texas (Fig. 3c). The Mountain West region and central Texas are notable for arid conditions in the present-day (including locations with present-day VPD of 2000 Pa and Δ VPD of 600 Pa (top right Fig. S7b)) that favor hydraulically resilient plants. By contrast, a distinct pattern of LAI loss along the East coast was present in a set of 11 models ('*' in Table S2; Fig. S10). The LAI loss matched patterns of decreased leaf area in both endmember allocation strategies in HOTTER.

Diagnosing potential hydraulic stress consequences of Earth system modeled leaf area

To evaluate the potential hydraulic stress consequences of ESM-projected LAI change, we used HOTTER as a complementary diagnostic for the ESMs and forced HOTTER with ESM-projected fractional LAI change as a boundary condition (see the [Materials and Methods](#) section). HOTTER model predictions indicated that the increased LAI in ESMs (realized as leaf area in HOTTER) would elevate chronic hydraulic stress substantially with an increased percent loss of conductivity in HOTTER by *c.* 12% in some places (99th percentile of the spatial distribution) in comparison with endmember allocation strategies. Endmember allocation strategies either collapse the change in hydraulic stress to zero (i.e. 'stress avoidance') or are centered near zero when allowed to maximize carbon gain where carbon assimilation is regulated by plant hydraulics (Figs 4, S11).

CO₂ fertilization effect across observations, HOTTER endmember allocation strategies, and Earth system models

We compared estimates of the CO₂ fertilization effect using HOTTER (including the endmember allocation strategies) and ESMs with observational estimations of the CO₂ fertilization effect on GPP in the literature. We found a similar CO₂ fertilization effect on GPP (without changing climate) across all of our allocation strategies in HOTTER (calculated as in (Walker *et al.*, 2021), see the [Materials and Methods](#) section). The spatial median of the CO₂ fertilization effect on GPP in HOTTER ranged from 0.30 ('stress avoidance') to 0.45 ('fixed leaf area') with

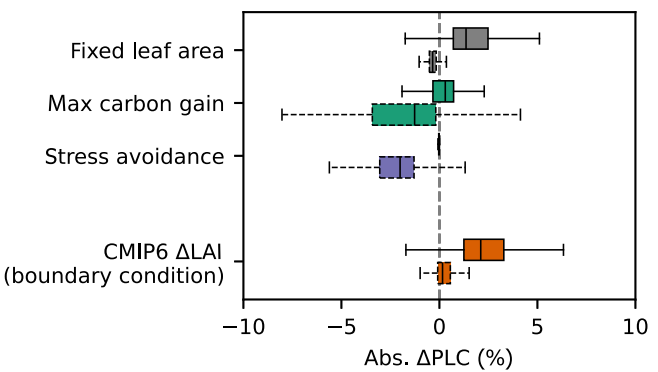


Fig. 4 Endmember allocation strategies both reduce hydraulic stress compared with no acclimation and Earth system model (ESM)-predicted leaf area change. Box plots represent the spatial distribution in the absolute change in PLC for future leaf area under 'fixed leaf area', 'max carbon gain', 'stress avoidance' (top), and 'CMIP6 boundary condition' (bottom). Run conditions are total climate plus increased atmosphere CO₂ (solid line boxplot) and CO₂ only (dashed line boxplot). Boxplots show the median (vertical line), 25th–75th quartiles (box), and 5th–95th (whiskers).

considerable overlap in their spatial distributions (Fig. 5). Overall, endmember allocation strategies tended to decrease the CO₂ fertilization effect compared with no acclimation, due to the widespread reduction in leaf area. Following endmember allocation strategies also generally increased the variance of the CO₂ fertilization effect across space compared with 'fixed leaf area' by strengthening the effect of climate variation on productivity through the climate effects on leaf area acclimation.

Similarly to HOTTER, the ESMs show a range of CO₂ fertilization responses across space (here the calculation of CO₂ fertilization also includes climate effects), but similar central tendencies to our optimality-based projections (Fig. 5, blue shaded box). Our comparison shows that, across techniques including optimality-derived estimates and ESMs, models project a substantially lower CO₂ fertilization effect on GPP compared with any of the theoretical or observationally derived proxies (Fig. 5, gray shaded box). However, it is important to note that caution should be taken in cross-comparing the estimations of the CO₂ fertilization effect size, especially observationally, as responses are derived from a diversity of scales and climate conditions. Furthermore, the range represented by HOTTER and ESM-projected CO₂ fertilization is generated by biogeographic variations in species and climate, while the range shown for observations is more strongly determined by uncertainty in measurement techniques.

Discussion

Avoiding future hydraulic stress misses maximizing carbon gain

HOTTER projected increased NPP under future climate conditions for both endmember allocation strategies, which qualitatively matches ESM projections, theory, and observed estimates about the effect of CO₂ fertilization on plant productivity

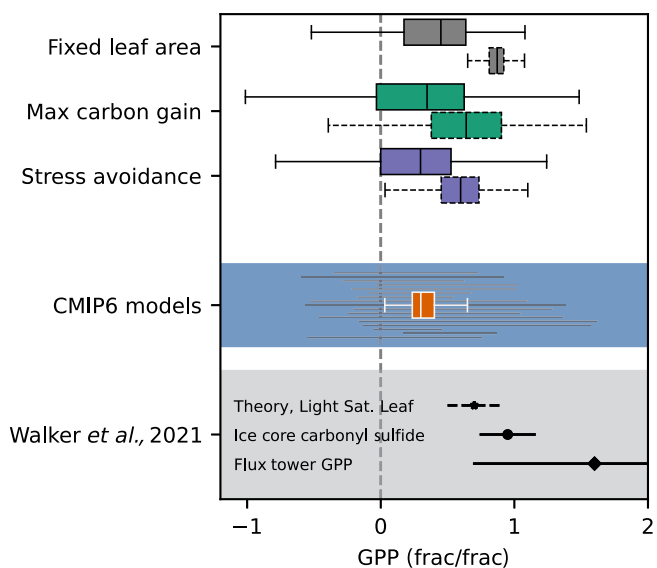


Fig. 5 Gross primary productivity (GPP) change is not distinguishable between leaf area allocation experiments and all overlap observations. CO₂ fertilization across endmember allocation strategies, CMIP6 models (blue shade), and observations ((Walker *et al.*, 2021), gray shade). White outlines and blue background designate GPP directly from the CMIP6 models with black lines showing the 5th–95th of individual models and the box plot showing the mean of the models, gray background designates CO₂ fertilization leaf level and observational estimates from (Walker *et al.*, 2021). Run conditions are total climate plus increased atmosphere CO₂ (solid line boxplot) and CO₂ only where available (dashed line boxplot). Boxplots show the median (vertical line), 25th–75th quartiles (box), and 5th–95th (whiskers).

(Gedalof & Berg, 2010; Piao *et al.*, 2013; Chi *et al.*, 2022). However, concomitant increases in hydraulic stress in the majority of regions following a ‘max carbon gain’ strategy have the potential to decrease fitness by increasing the risk of hydraulic failure and mortality along with co-occurring mortality drivers such as wildfire and pest and pathogen outbreaks (Park Williams *et al.*, 2013; Anderegg *et al.*, 2015; Adams *et al.*, 2017). The real cost in terms of fitness of an increase in chronic hydraulic stress on order of a few percent remains unknown but represents a shift in the baseline, with potential for degraded tree functionality, for example through ‘cavitation fatigue’ (Hacke *et al.*, 2001) (Anderegg *et al.*, 2015). On the time scales of a single drought, observations of leaf shedding in response to drought conditions show how leaf allocation dynamics operate to help avoid hydraulic damage, with a benefit to overall plant health (Sabot *et al.*, 2022).

From a carbon cycle perspective, higher NPP could support increased plant growth and potentially increase fitness if not accounting for the mortality risk of increased hydraulic stress (Piao *et al.*, 2020). The relatively small value of NPP_{miss} in the context of potentially costly and catastrophic hydraulic damage, highlights that stress preservation and/or minimization may be an important plant allocation strategy that should be explored further through a combined modeling and empirical approach.

HOTTER predicts that acclimation following either endmember allocation strategy benefits the tree’s carbon balance. This

suggests that forests could go through major structural changes regardless of whether they are protecting against hydraulic damage or seeking to maximize their carbon gain under climate change conditions. Additionally, model projections indicate that different leaf area acclimation strategies may have as large of an effect on plant carbon and water status as a shift in species composition (represented here as a shift in the functional trait P50). The modulation of allocation strategy by hydraulic traits suggests that changes in forest structure will be dependent on species such that future conditions have the potential to reshape ecosystems through both competition and acclimation.

Other carbon allocation optimization could co-limit leaf area increase

The systematic difference between the widespread leaf area decreases following endmember allocation strategies in HOTTER and the future uncertainty in ESM LAI aligns with the uncertainty in prognostic leaf area (Zhao *et al.*, 2020; Song *et al.*, 2021; Yang *et al.*, 2022) and the spread in the sensitivity of ESM LAI to interannual climate variations (Quentin & Swann, 2018). The agreement between HOTTER and a weak majority of ESMs on leaf area decrease is primarily limited to the relatively wet North East region of the United States where we would expect processes tangential to plant hydraulics to be limiting (e.g. the biogeochemistry of productivity).

In many of the ESMs showing decrease, we find a common thread of carbon allocation that is responsive to resource limitations (e.g. soil moisture, nitrogen, and light). For example, model *BCC_BCC-CSM2-MR* includes a phenology model with a dynamic ‘cost-gain’ carbon allocation scheme for canopy leaf area which shifts carbon allocation to stem or roots depending on resource limitations such as drier soils (Arora & Boer, 2005; Wu *et al.*, 2019). This ‘cost-gain’ approach is also used in the two versions of *CanESM5* that showed LAI decreases. Generally, including carbon allocation that is responsive to resource limitation can limit leaf area increases. In *EC-Earth-Consortium_EC-Earth3-Veg-LR*, nitrogen limitation allows for a dynamic shift of carbon allocation from foliage to roots (Smith *et al.*, 2014) and *MOHC_UKESM1-0-LL* includes carbon attribution based on competition and height (Harper *et al.*, 2018).

While our experiments do not include prognostic soil moisture, nitrogen limitation, or competition we offer several hypotheses on how these processes may interact with plant hydraulics and allocation strategies implemented in HOTTER. We expect that soil moisture feedback would only accentuate the decrease in leaf area as both the ‘max carbon gain’ and (to a lesser extent) the ‘stress avoidance’ allocation strategies both predict increases in transpiration (Fig. S13). This increased transpiration would decrease soil water potential in the absence of major changes in precipitation. Including a nitrogen cycle and nitrogen limitation impacts on per leaf canopy productivity would likely also act to limit leaf area, potentially also decreasing model-predicted hydraulic stress where nitrogen is limiting. Finally, investing more carbon in stem area and height due to competition for light could both limit leaf area and create a longer hydraulic path

which would increase stress (or also limit leaf area) (Trugman *et al.*, 2018; Liu *et al.*, 2019). Indeed, the decrease in future leaf area projected by our endmember allocation strategies can be most precisely interpreted as a decrease in the ratio of leaf area to stem area, not necessarily as solely decreases in leaf area. Increasing the stem area through growth could theoretically support the hydraulic demand of an increase in leaf area, however, increased stem area would also increase respiration costs per leaf area – potentially limiting the benefit to NPP.

Additional mechanisms and forms of acclimation may also interact with changes in carbon allocation to leaf area. For example, leaf-to-crown scaling and self-shading may be import in high leaf area regions such as the Northeast. While HOTTER employs a purposefully parsimonious linear scaling between carbon and water fluxes and crown leaf area, many ESMs account for increased shading due to higher leaf area per canopy area (i.e. LAI) (Sellers, 1985) (Notes S2). Accounting for shading would further reduce the benefit of increased leaf area, potentially resulting in a co-limitation with hydraulic stress. This could reduce both the hydraulic stress in ‘present-day’ HOTTER runs and the hydraulic stress under future conditions. Leaf area is also not the only part of plants that can acclimate to future conditions. For example, $V_{c,\max 25}$ has been shown to decrease with increased CO_2 and temperature (on order of 10–20% with a doubling of CO_2 concentrations) (Ainsworth & Long, 2005; Dong *et al.*, 2022). Relative to a scenario where $V_{c,\max 25}$ does not acclimate, acclimation would reduce the productivity of trees and likely relieve some hydraulic stress, given that this would decrease transpiration. We found that a 20% decrease in $V_{c,\max 25}$ – applied in HOTTER – allows for a relative increase in leaf area for a carbon maximization strategy, but does not change the overall results of a general leaf area decrease (Fig. S6). Finally, acclimation of respiration to increasing temperatures and productivity would likely allow for increased leaf area following a ‘max carbon gain’ strategy (H. Wang *et al.*, 2020).

Unexplored Earth system effects with future decreased leaf area

HOTTER-projected changes allow us to hypothesize about broader-scale land surface dynamics associated with ESM projections. The difference between broad-scale leaf area decreases (HOTTER predicted) or the more commonly studied leaf area increases (ESM-predicted) could have widespread consequences for the terrestrial carbon cycle, surface energy budget, and global circulation patterns. In particular, this would result in a strong overestimation of plant growth and future terrestrial carbon storage in the ESMs when the impacts of stress-driven mortality are not accounted for, as is true of many of the current generation of ESMs. These implications are not only important from a biological perspective, but impact societal strategies to get to net zero emissions (Coffield *et al.*, 2021). Meanwhile, vegetation biomass and leaf area are also key determinants of surface albedo and evaporative fraction which are a critical component in the Earth’s energy balance, water cycles, and atmospheric circulation through the surface energy budget (Bonan, 2008). In ESMs, a decrease in leaf area could have impacts on land-atmospheric feedbacks,

global climate temperature sensitivity, and atmospheric water vapor (Swann *et al.*, 2010; Alkama & Cescatti, 2016; Zarakas *et al.*, 2020). Finally, changes in leaf area in the mid-latitudes – including our study region – have been linked to changes in global circulation with teleconnections shifting precipitation in the tropics (Swann *et al.*, 2012). Considering the ecological, carbon cycle, and Earth system implications of these studies – with ESMs that overwhelmingly predict leaf area increase with climate change – the understudied impacts of combined high CO_2 and concomitant climate change with a weakening land carbon sink and decreased forest presence are all but guaranteed to be an area of importance for the future of the Earth system.

Diagnosing potentially lethal hydraulic stress in Earth system model leaf area projections

While HOTTER does not represent demographic processes such as growth and mortality, inferences about future allocation strategies and hydraulic stress complement information on the terrestrial biosphere derived from global-scale ESMs. Though efforts are underway to include more realistic plant hydraulic and mortality mechanisms in ESMs (Kennedy *et al.*, 2019; De Kauwe *et al.*, 2020), ESMs have yet to surmount the challenge of scaling an organ-level understanding of plant hydraulic processes to a land surface model grid cell that is 50–100 km along one side. Thus, it remains to be determined what the combined effect of these stressors will be on mortality and what the net effect will be on terrestrial carbon storage (Arora & Melton, 2018; Lemordant *et al.*, 2018; Bonan *et al.*, 2019; Anderegg *et al.*, 2022; Cano *et al.*, 2022; Wu *et al.*, 2023). However, we can use HOTTER as a diagnostic to better understand the potential hydraulic consequences of the ESM’s predictions of the terrestrial biosphere. For example, HOTTER-projected increase in PLC due to increases in leaf area that are representative of ESMs under climate change scenarios could accelerate mortality rates, increasing carbon turnover and offsetting carbon gains from increased productivity associated with CO_2 fertilization (Anderegg *et al.*, 2015, 2022; Quetin *et al.*, 2023; Wu *et al.*, 2023).

Results from applying ESM leaf area change as a boundary condition in HOTTER suggest that the ESM’s projected leaf increase – responding to higher productivity and available GPP – would be a strong leaf area overshoot in terms of hydraulic stress leading to stress-driven mortality (e.g. Quetin *et al.*, 2023; Figs 4, S12). While it is possible that some changes in forest structure could help alleviate hydraulic stress, forest structure is the complex result of decades to centuries of forest management, and ecological factors of recruitment, growth and mortality, and thus represents additional complexity for all future projections (Eagleson, 1982; Bradford John *et al.*, 2022).

Observations of the CO_2 fertilization effect have limited ability to distinguish between HOTTER endmember allocation strategies and Earth system models

The response of plants to increased atmospheric concentrations of CO_2 continues to be a large uncertainty for the future carbon cycle

and a focus of intensive field experiments (King *et al.*, 2004; O'Sullivan *et al.*, 2022). Model-derived projections for estimating the CO₂ fertilization effect on GPP have come under increased scrutiny for potentially unrealistic and overoptimistic effect sizes (W. Li *et al.*, 2018; S. Wang *et al.*, 2020). We examined observational estimations of the CO₂ fertilization effect on GPP to see whether these observations could provide a constraint on which – if either – model-predicted allocation strategy most realistically reproduce plant responses to environmental and CO₂ perturbations. Despite being a focus in the literature for its potential to constrain future model prediction, we found that the strength of the CO₂ fertilization effect on GPP has little ability to discriminate between endmember allocation strategies or between our endmember approaches and ESM projections (Fig. 5). The comparison highlights the difficulty of using observationally derived proxies (and leaf-level theory) – including flux tower measurements, global carbonyl sulfide from ice cores, and theory for light saturated leaves – in constraining model projections.

Conclusion

We quantified the carbon gain and hydraulic stress consequences of two potentially endmember allocation strategies (maximizing carbon gain or conserving hydraulic stress), implemented in a trait-based physiological tree model with plant hydraulics under future climate change conditions. We found that the 'stress avoidance' allocation strategy missed out on up to 26% of NPP in some locations compared with the carbon maximization strategy. Furthermore, the observed fertilization effect on GPP had little ability to discriminate between endmember allocation strategies or between our endmember approaches and ESM projections. This fact is important to consider given that the literature focuses on the CO₂ fertilization effect on GPP as a potential constraint on terrestrial biosphere predictions. We provide evidence that GPP may not be the most relevant ecological or biogeochemical diagnostic to consider, and also likely does not provide sufficient information about climate impacts on terrestrial carbon cycle dynamics, given the importance of both carbon assimilation and respiration. Finally, ESMs – our state-of-the-science tools for understanding climate change impacts on the Earth system – overwhelmingly project leaf area increases due to increased photosynthesis with higher atmospheric CO₂. However, our endmember allocation strategies show that plant hydraulics may play an important role in limiting leaf area – and ultimately plant biomass – increases. Conversely, if ESM-projected leaf areas are realized, our results suggest increases in hydraulic stress connected to increased mortality. Either path would impact the carbon sink and Earth system, with reduced leaf area effectively downregulating photosynthesis and changing land-atmosphere feedbacks, or increased hydraulic stress leading to increased carbon turnover associated with mortality, disturbance, and demographic changes.

Acknowledgements

This research was funded by the NSF (grant no.: 2003205). ATT acknowledges funding from the NSF (grant nos.: 2017949 and

2216855), the USDA National Institute of Food and Agriculture, Agricultural and Food Research Initiative Competitive Programme (grant no.: 2018-67012-31496).

Competing interests

None declared.

Author contributions

GRQ and ATT designed the study with input from LDLA and IB. GRQ performed the analysis. GRQ and ATT wrote the paper, with all authors contributing comments.

ORCID

Leander D. L. Anderegg  <https://orcid.org/0000-0002-5144-7254>

Indra Boving  <https://orcid.org/0000-0002-2176-2819>

Gregory R. Quetin  <https://orcid.org/0000-0002-7884-5332>

Anna T. Trugman  <https://orcid.org/0000-0002-7903-9711>

Data availability

The data that support the findings of this study are publicly available online at [10.6084/m9.figshare.24415966](https://doi.org/10.6084/m9.figshare.24415966). All other datasets used in this analysis are publicly available. The analysis code supporting this publication is available online on Figshare at [10.6084/m9.figshare.24415972](https://doi.org/10.6084/m9.figshare.24415972).

References

- Adams HD, Zeppel MJB, Anderegg WRL, Hartmann H, Landhäusser SM, Tissue DT, Huxman TE, Hudson PJ, Franz TE, Allen CD *et al.* 2017. A multi-species synthesis of physiological mechanisms in drought-induced tree mortality. *Nature Ecology & Evolution* 1: 1285–1291.
- Ainsworth EA, Long SP. 2005. What have we learned from 15 years of free-air CO₂ enrichment (FACE)? A meta-analytic review of the responses of photosynthesis, canopy properties and plant production to rising CO₂. *New Phytologist* 165: 351–372.
- Alkama R, Cescatti A. 2016. Biophysical climate impacts of recent changes in global forest cover. *Science* 351: 600–604.
- Allen CD, Breshears DD, McDowell NG. 2015. On underestimation of global vulnerability to tree mortality and forest die-off from hotter drought in the Anthropocene. *Ecosphere* 6(8): art129.
- Anderegg WRL, Chegwidden OS, Badgley G, Trugman AT, Cullenward D, Abatzoglou JT, Hicke JA, Freeman J, Hamman JJ. 2022. Future climate risks from stress, insects and fire across US forests. *Ecology Letters* 25: 1510–1520.
- Anderegg WRL, Flint A, Huang C, Flint L, Berry JA, Davis FW, Sperry JS, Field CB. 2015. Tree mortality predicted from drought-induced vascular damage. *Nature Geoscience* 8: 367–371.
- Arora VK, Boer GJ. 2005. A parameterization of leaf phenology for the terrestrial ecosystem component of climate models. *Global Change Biology* 11: 39–59.
- Arora VK, Melton JR. 2018. Reduction in global area burned and wildfire emissions since 1930s enhances carbon uptake by land. *Nature Communications* 9: 1326.
- Baldocchi DD, Xu L. 2007. What limits evaporation from Mediterranean oak woodlands – The supply of moisture in the soil, physiological control by plants or the demand by the atmosphere? *Advances in Water Resources* 30: 2113–2122.

Battipaglia G, Sauer M, Cherubini P, Calfapietra C, McCarthy HR, Norby RJ, Francesca Cotrufo M. 2013. Elevated CO₂ increases tree-level intrinsic water use efficiency: insights from carbon and oxygen isotope analyses in tree rings across three forest FACE sites. *New Phytologist* 197: 544–554.

Bonan GB. 2008. Forests and climate change: forcings, feedbacks, and the climate benefits of forests. *Science* 320: 1444–1449.

Bonan GB, Lombardozzi DL, Wieder WR, Oleson KW, Lawrence DM, Hoffman FM, Collier N. 2019. Model structure and climate data uncertainty in historical simulations of the terrestrial carbon cycle (1850–2014). *Global Biogeochemical Cycles* 33: 1310–1326.

Bradford John B, Shriver RK, Robles MD, McCauley LA, Woolley TJ, Andrews CA, Crimmins M, Bell DM. 2022. Tree mortality response to drought-density interactions suggests opportunities to enhance drought resistance. *Journal of Applied Ecology* 59: 549–559.

Cano IM, Sheviakova E, Malyshov S, John JG, Yu Y, Smith B, Pacala SW. 2022. Abrupt loss and uncertain recovery from fires of Amazon forests under low climate mitigation scenarios. *Proceedings of the National Academy of Sciences, USA* 119: e2203200119.

Chen JM, Ju W, Ciais P, Viovy N, Liu R, Liu Y, Lu X. 2019. Vegetation structural change since 1981 significantly enhanced the terrestrial carbon sink. *Nature Communications* 10: 4259.

Chi C, Riley WJ, Colin PI, Keenan TF. 2022. CO₂ fertilization of terrestrial photosynthesis inferred from site to global scales. *Proceedings of the National Academy of Sciences, USA* 119: e2115627119.

Coffield SR, Hemes KS, Koven CD, Goulden ML, Randerson JT. 2021. Climate-driven limits to future carbon storage in California's wildland ecosystems. *AGU Advances* 2: e2021AV000384.

De Kauwe MG, Medlyn BE, Ukkola AM, Ma M, Sabot MEB, Pitman AJ et al. 2020. Identifying areas at risk of drought-induced tree mortality across South-Eastern Australia. *Global Change Biology* 26: 5716–5733.

De Kauwe MG, Medlyn BE, Zaehle S, Walker AP, Dietze MC, Wang Y-P, Luo Y, Jain AK, E-Masri B, Hickler T et al. 2014. Where does the carbon go? A model–data intercomparison of vegetation carbon allocation and turnover processes at two temperate forest free-air CO₂ enrichment sites. *New Phytologist* 203: 883–899.

Deans RM, Brodribb TJ, Busch FA, Farquhar GD. 2020. Optimization can provide the fundamental link between leaf photosynthesis, gas exchange and water relations. *Nature Plants* 6: 1116–1125.

Domec J-C, Smith DD, McCulloch KA. 2017. A synthesis of the effects of atmospheric carbon dioxide enrichment on plant hydraulics: implications for whole-plant water use efficiency and resistance to drought: CO₂ effects on plant hydraulics. *Plant, Cell & Environment* 40: 921–937.

Dong N, Wright IJ, Chen JM, Luo X, Wang H, Keenan TF, Smith NG, Prentice IC. 2022. Rising CO₂ and warming reduce global canopy demand for nitrogen. *New Phytologist* 235: 1692–1700.

Eagleson PS. 1982. Ecological optimality in water-limited natural soil–vegetation systems: 1. Theory and hypothesis. *Water Resources Research* 18: 325–340.

Eller CB, Rowland L, Oliveira RS, Bittencourt PRL, Barros FV, da Costa ACL, Meir P, Friend AD, Mencuccini M, Sitch S et al. 2018. Modelling tropical forest responses to drought and El Niño with a stomatal optimization model based on xylem hydraulics. *Philosophical Transactions of the Royal Society of London. Series B: Biological Sciences* 373: 20170315.

Eyring V, Bony S, Meehl GA, Senior CA, Stevens B, Stouffer RJ, Taylor KE. 2016. Overview of the Coupled Model Intercomparison Project Phase 6 (CMIP6) experimental design and organization. *Geoscientific Model Development* 9: 1937–1958.

Franklin O, Harrison SP, Dewar R, Farrar CE, Brännström Å, Dieckmann U, Pietsch S, Falster D, Cramer W, Loreau M et al. 2020. Organizing principles for vegetation dynamics. *Nature Plants* 6: 444–453.

Franklin O, Johansson J, Dewar RC, Dieckmann U, McMurtie RE, Brannstrom A, Dybinski R. 2012. Modeling carbon allocation in trees: a search for principles. *Tree Physiology* 32: 648–666.

Franks PJ, Adams MA, Amthor JS, Barbour MM, Berry JA, Ellsworth DS, Farquhar GD, Ghannoum O, Lloyd J, McDowell N et al. 2013. Sensitivity of plants to changing atmospheric CO₂ concentration: from the geological past to the next century. *New Phytologist* 197: 1077–1094.

Gedalof Z, Berg AA. 2010. Tree ring evidence for limited direct CO₂ fertilization of forests over the 20th century: limited CO₂ fertilization of forests. *Global Biogeochemical Cycles* 24: GB3027. doi: 10.1029/2009GB003699.

Gillespie AJ. 1999. Rationale for a national annual forest inventory program. *Journal of Forestry* 97: 16–20.

Grossiord C, Buckley TN, Cernusak LA, Novick KA, Poulter B, Siegwolf RTW, Sperry JS, McDowell NG. 2020. Plant responses to rising vapor pressure deficit. *New Phytologist* 226: 1550–1566.

Hacke UG, Sperry JS, Pockman WT, Davis SD, McCulloch KA. 2001. Trends in wood density and structure are linked to prevention of xylem implosion by negative pressure. *Oecologia* 126: 457–461.

Harper AB, Wiltshire AJ, Cox PM, Friedlingstein P, Jones CD, Mercado LM, Sitch S, Williams K, Duran-Rojas C. 2018. Vegetation distribution and terrestrial carbon cycle in a carbon cycle configuration of JULES4.6 with new plant functional types. *Geoscientific Model Development* 11: 2857–2873.

Harrison SP, Cramer W, Franklin O, Prentice IC, Wang H, Brännström Å, de Boer H, Dieckmann U, Joshi J, Keenan TF et al. 2021. Eco-evolutionary optimality as a means to improve vegetation and land-surface models. *New Phytologist* 231: 2125–2141.

Hartmann H, Bahn M, Carbone M, Richardson AD. 2020. Plant carbon allocation in a changing world – challenges and progress: introduction to a Virtual Issue on carbon allocation. *New Phytologist* 227: 981–988.

Hartmann H, Moura CF, Anderegg WRL, Ruehr NK, Salmon Y, Allen CD, Arndt SK, Breshears DD, Davi H, Galbraith D et al. 2018. Research frontiers for improving our understanding of drought-induced tree and forest mortality. *New Phytologist* 218: 15–28.

Hölttä T, Mencuccini M, Nikinmaa E. 2011. A carbon cost-gain model explains the observed patterns of xylem safety and efficiency: a carbon gain-cost model for xylem structure. *Plant, Cell & Environment* 34: 1819–1834.

Humphrey V, Berg A, Ciais P, Gentile P, Jung M, Reichstein M, Seneviratne SI, Frankenberg C. 2021. Soil moisture–atmosphere feedback dominates land carbon uptake variability. *Nature* 592: 65–69.

Joshi J, Stocker BD, Hofhansl F, Zhou S, Dieckmann U, Prentice IC. 2022. Towards a unified theory of plant photosynthesis and hydraulics. *Nature Plants* 8: 1304–1316.

Keeling R, Graven HD, Welp LR, Resplandy L, Bi J, Piper SC et al. 2017. Atmospheric evidence for a global secular increase in carbon isotopic discrimination of land photosynthesis. *Proceedings of the National Academy of Sciences, USA* 114: 10361–10366.

Keeling R, Piper S, Bollenbacher A, Walker J. 2009. *Atmospheric carbon dioxide record from Mauna Loa (1958–2008)*. Oak Ridge, TN, USA: Carbon Dioxide Information Analysis Center (CDIAC). [WWW document] URL www.esrl.noaa.gov/gmd/ccgg/trends/ [accessed 3 January 2024].

Kennedy D, Swenson S, Oleson KW, Lawrence DM, Fisher R, Lola Da Costa AC, Gentile P. 2019. Implementing plant hydraulics in the community land model, version 5. *Journal of Advances in Modeling Earth Systems* 11: 485–513.

King JS, Hanson PJ, Bernhardt E, DeAngelis P, Norby RJ, Pregitzer KS. 2004. A multiyear synthesis of soil respiration responses to elevated atmospheric CO₂ from four forest FACE experiments. *Global Change Biology* 10: 1027–1042.

Lemordant L, Gentile P, Swann AS, Cook BI, Scheff J. 2018. Critical impact of vegetation physiology on the continental hydrologic cycle in response to increasing CO₂. *Proceedings of the National Academy of Sciences, USA* 115: 4093–4098.

Levionnois S, Ziegler C, Jansen S, Calvet E, Coste S, Stahl C, Salmon C, Delzon S, Guichard C, Heuret P. 2020. Vulnerability and hydraulic segmentations at the stem–leaf transition: coordination across Neotropical trees. *New Phytologist* 228: 512–524.

Li B, Beaudoing H, Rodell M. 2020. *GLDAS catchment land surface model L4 daily 0.25 × 0.25 degree GRACE-DAI V2.2*, vol. 16. Greenbelt, MD, USA: Goddard Earth Sciences Data and Information Services Center (GES DISC), 1–32.

Li B, Rodell M, Kumar S, Beaudoing HK, Getirana A, Zaitchik BF, de Goncalves LG, Cossetin C, Bhanja S, Mukherjee A et al. 2019. Global GRACE data assimilation for groundwater and drought monitoring: advances and challenges. *Water Resources Research* 55: 7564–7586.

Li Q, Lu X, Wang Y, Huang X, Cox PM, Luo Y. 2018. Leaf area index identified as a major source of variability in modeled CO₂ fertilization. *Biogeosciences* 15: 6909–6925.

Li W, Ciais P, Wang Y, Yin Y, Peng S, Zhu Z, Bastos A, Yue C, Ballantyne AP, Broquet G *et al.* 2018. Recent changes in global photosynthesis and terrestrial ecosystem respiration constrained from multiple observations. *Geophysical Research Letters* 45: 1058–1068.

Liu H, Gleason SM, Hao G, Hua L, He P, Goldstein G, Ye Q. 2019. Hydraulic traits are coordinated with maximum plant height at the global scale. *Science Advances* 5(2): eaav1332.

Mathias JM, Trugman AT. 2022. Climate change impacts plant carbon balance, increasing mean future carbon use efficiency but decreasing total forest extent at dry range edges. *Ecology Letters* 25: 498–508.

Mooney H, Gulmon S. 1979. Environmental and evolutionary constraints on the photosynthetic characteristics of higher plants. In: *Topics in plant population biology*. London, UK: Palgrave, 316–337.

Nadal-Sala D, Grote R, Birami B, Knüver T, Rehschuh R, Schwarz S, Ruehr NK. 2021. Leaf shedding and non-stomatal limitations of photosynthesis mitigate hydraulic conductance losses in scots pine saplings during severe drought stress. *Frontiers in Plant Science* 12: 715127.

O'Neill BC, Tebaldi C, Van Vuuren DP, Eyring V, Friedlingstein P, Hurtt G *et al.* 2016. The scenario model intercomparison project (ScenarioMIP) for CMIP6. *Geoscientific Model Development* 9: 3461–3482.

O'Sullivan M, Friedlingstein P, Sitch S, Anthoni P, Arneth A, Arora VK *et al.* 2022. Process-oriented analysis of dominant sources of uncertainty in the land carbon sink. *Nature Communications* 13: 4781.

Park Williams A, Allen CD, Macalady AK, Griffin D, Woodhouse CA, Meko DM, Swetnam TW, Rauscher SA, Seager R, Grissino-Mayer HD *et al.* 2013. Temperature as a potent driver of regional forest drought stress and tree mortality. *Nature Climate Change* 3: 292–297.

Piao S, Sitch S, Ciais P, Friedlingstein P, Peylin P, Wang X, Ahlström A, Anav A, Canadell JG, Cong N *et al.* 2013. Evaluation of terrestrial carbon cycle models for their response to climate variability and to CO₂ trends. *Global Change Biology* 19: 2117–2132.

Piao S, Wang X, Park T, Chen C, Lian X, He Y, Bjerke JW, Chen A, Ciais P, Tømmervik H *et al.* 2020. Characteristics, drivers and feedbacks of global greening. *Nature Reviews Earth and Environment* 1: 14–27.

Pivovaroff AL, Pasquini SC, De Guzman ME, Alstad KP, Stemke JS, Santiago LS. 2016. Multiple strategies for drought survival among woody plant species. *Functional Ecology* 30: 517–526.

Pivovaroff AL, Sack L, Santiago LS. 2014. Coordination of stem and leaf hydraulic conductance in southern California shrubs: a test of the hydraulic segmentation hypothesis. *New Phytologist* 203: 842–850.

Potapov P, Li X, Hernandez-Serna A, Tyukavina A, Hansen MC, Kommareddy A, Pickens A, Turubanova S, Tang H, Silva CE *et al.* 2021. Mapping global forest canopy height through integration of GEDI and Landsat data. *Remote Sensing of Environment* 253: 112165.

Quentin GR, Anderegg LDL, Boving I, Anderegg WRL, Trugman AT. 2023. Observed forest trait velocities have not kept pace with hydraulic stress from climate change. *Global Change Biology* 29: 5415–5428. doi: 10.1111/gcb.16847.

Quentin GR, Swann ALS. 2018. Sensitivity of leaf area to interannual climate variation as a diagnostic of ecosystem function in CMIP5 carbon cycle models. *Journal of Climate* 31: 8607–8625.

Rowland L, Ramírez-Valiente J, Hartley IP, Mencuccini M. 2023. How woody plants adjust above- and below-ground traits in response to sustained drought. *New Phytologist* 239: 1173–1189.

Sabot MEB, De Kauwe MG, Pitman AJ, Ellsworth DS, Medlyn BE, Calderaru S *et al.* 2022. Predicting resilience through the lens of competing adjustments to vegetation function. *Plant, Cell & Environment* 45: 2744–2761.

Sanchez-Martinez P, Martínez-Vilalta J, Dexter KG, Segovia RA, Mencuccini M. 2020. Adaptation and coordinated evolution of plant hydraulic traits. *Ecology Letters* 23: 1599–1610.

Schlesinger WH, Jasechko S. 2014. Transpiration in the global water cycle. *Agricultural and Forest Meteorology* 189–190(0): 115–117.

Sellers PJ. 1985. Canopy reflectance, photosynthesis and transpiration. *International Journal of Remote Sensing* 6: 1335–1372.

Smith B, Wårldin D, Arneth A, Hickler T, Leadley P, Siltberg J, Zaehle S. 2014. Implications of incorporating N cycling and N limitations on primary production in an individual-based dynamic vegetation model. *Biogeosciences* 11: 2027–2054.

Song X, Wang D-Y, Li F, Zeng X-D. 2021. Evaluating the performance of CMIP6 Earth system models in simulating global vegetation structure and distribution. *Advances in Climate Change Research* 12: 584–595.

Swann ALS, Fung IY, Chiang JCH. 2012. Mid-latitude afforestation shifts general circulation and tropical precipitation. *Proceedings of the National Academy of Sciences, USA* 109: 712–716.

Swann ALS, Fung IY, Levis S, Bonan GB, Doney SC. 2010. Changes in Arctic vegetation amplify high-latitude warming through the greenhouse effect. *Proceedings of the National Academy of Sciences, USA* 107: 1295–1300.

Trugman AT, Anderegg LDL, Shaw JD, Anderegg WRL. 2020. Trait velocities reveal that mortality has driven widespread coordinated shifts in forest hydraulic trait composition. *Proceedings of the National Academy of Sciences, USA* 117: 8532–8538.

Trugman AT, Anderegg LDL, Sperry JS, Wang Y, Venturas M, Anderegg WRL. 2019. Leveraging plant hydraulics to yield predictive and dynamic plant leaf allocation in vegetation models with climate change. *Global Change Biology* 25: 4008–4021.

Trugman AT, Dettman M, Bartlett MK, Medvigy D, Anderegg WRL, Schwalm C, Schaffer B, Pacala SW. 2018. Tree carbon allocation explains forest drought-kill and recovery patterns. *Ecology Letters* 21: 1552–1560.

Walker AP, De Kauwe MG, Bastos A, Belmecheri S, Georgiou K, Keeling RF *et al.* 2021. Integrating the evidence for a terrestrial carbon sink caused by increasing atmospheric CO₂. *New Phytologist* 229: 2413–2445.

Wang H, Atkin OK, Keenan TF, Smith NG, Wright IJ, Bloomfield KJ, Kattge J, Reich PB, Prentice IC. 2020. Acclimation of leaf respiration consistent with optimal photosynthetic capacity. *Global Change Biology* 26: 2573–2583.

Wang S, Zhang Y, Ju W, Chen JM, Ciais P, Cescatti A *et al.* 2020. Recent global decline of CO₂ fertilization effects on vegetation photosynthesis. *Science* 370(6522): 1295–1300.

Wolf A, Anderegg WRL, Pacala SW. 2016. Optimal stomatal behavior with competition for water and risk of hydraulic impairment. *Proceedings of the National Academy of Sciences, USA* 113: E7222–E7230.

Wolfe BT, Sperry JS, Kursar TA. 2016. Does leaf shedding protect stems from cavitation during seasonal droughts? A test of the hydraulic fuse hypothesis. *New Phytologist* 212: 1007–1018.

Wu C, Coffield SR, Goulden ML, Randerson JT, Trugman AT, Anderegg WRL. 2023. Uncertainty in US forest carbon storage potential due to climate risks. *Nature Geoscience* 16: 422–429.

Wu T, Lu Y, Fang Y, Xin X, Li L, Li W, Jie W, Zhang J, Liu Y, Zhang L *et al.* 2019. The Beijing Climate Center Climate System Model (BCC-CSM): the main progress from CMIP5 to CMIP6. *Geoscientific Model Development* 12: 1573–1600.

Xu X, Medvigy D, Powers JS, Becknell JM, Guan K. 2016. Diversity in plant hydraulic traits explains seasonal and inter-annual variations of vegetation dynamics in seasonally dry tropical forests. *New Phytologist* 212: 80–95.

Yang H, Ciais P, Frappart F, Li X, Brandt M, Fensholt R, Fan L, Saatchi S, Besnard S, Deng Z *et al.* 2023. Global increase in biomass carbon stock dominated by growth of northern young forests over past decade. *Nature Geoscience* 16: 886–892.

Yang R, Wang J, Zeng N, Sitch S, Tang W, McGrath MJ, Cai Q, Liu D, Lombardozzi D, Tian H *et al.* 2022. Divergent historical GPP trends among state-of-the-art multi-model simulations and satellite-based products. *Earth System Dynamics* 13: 833–849.

Yuan S, Quiring SM, Leasor ZT. 2021. Historical changes in surface soil moisture over the contiguous United States: an assessment of CMIP6. *Geophysical Research Letters* 48(1): e2020GL089991.

Zarakas CM, Swann ALS, Laguë MM, Armour KC, Randerson JT. 2020. Plant physiology increases the magnitude and spread of the transient climate response to CO₂ in CMIP6 earth system models. *Journal of Climate* 33: 8561–8578.

Zhao Q, Zhu Z, Zeng H, Zhao W, Myneni RB. 2020. Future greening of the Earth may not be as large as previously predicted. *Agricultural and Forest Meteorology* 292–293: 108111.

Supporting Information

Additional Supporting Information may be found online in the Supporting Information section at the end of the article.

Fig. S1 HOTTER integrates tree productivity, water use, and the hydraulic stress across the soil-atmosphere continuum.

Fig. S2 No leaf area acclimation has a high carbon cost and large hydraulic stress increases.

Fig. S3 The distribution across the US for GPP, NPP, and PLC for different allocation strategies.

Fig. S4 The regional range of P50 values significantly impacts the carbon missed out on for 'stress avoidance' in many regions.

Fig. S5 Leaf area predicted by HOTTER for the continental U.S.

Fig. S6 The percent change in leaf area with a 20% reduction in $V_{c,\max25}$ under future conditions for the 'max carbon gain' allocation strategy.

Fig. S7 Maximizing carbon gain limits leaf area more than stress avoidance in regions with low present-day vapor pressure deficit.

Fig. S8 Histogram of the difference in the percent leaf area change between the endmember allocation strategies of 'stress avoidance' vs 'max carbon gain'.

Fig. S9 The model and anomaly for the difference in leaf area change between endmember allocation strategies of stress avoidance and maximum carbon gain.

Fig. S10 Maps of the percent leaf area index change for each model included in CMIP6 that was used in the analysis.

Fig. S11 There is large uncertainty in the percent change in leaf area across the Earth system models by 2100.

Fig. S12 Net primary productivity and percent loss of conductance from running HOTTER with the fractional leaf area change from the mean of the CMIP6 Earth system models.

Fig. S13 Transpiration generally increases under conditions for most leaf area strategies.

Methods S1 HOTTER-SOX model description.

Methods S2 Software.

Notes S1 Canopy scaling and the difference between HOTTER leaf area and leaf area index.

Notes S2 Max carbon gain, more than stress avoidance limits future leaf area in some regions.

Table S1 HOTTER key inputs and outputs. Reproduced from Quetin *et al.* (2023).

Table S2 List of CMIP6 models that were analyzed and the percent of grid points with LAI decrease in the future.

Table S3 The mean environments for different quadrants as seen in Fig. 2.

Table S4 The variance explained by different combinations of predictors in a linear model of the difference in leaf area change between endmember allocation strategies.

Please note: Wiley is not responsible for the content or functionality of any Supporting Information supplied by the authors. Any queries (other than missing material) should be directed to the *New Phytologist* Central Office.